Atmosphere–Ocean Mechanisms of Climate Anomalies in the Angola–Tropical Atlantic Sector

ANTHONY C. HIRST AND STEFAN HASTENRATH

Department of Meteorology, The University of Wisconsin, Madison 53706

(Manuscript received 25 October 1982, in final form 7 April 1983)

ABSTRACT

Interannual variations in the large-scale atmospheric and oceanic fields over the tropical Atlantic are studied in relation to rainfall anomalies on the Angola coast. Departure patterns are constructed by stratification with respect to extremely dry and wet years and by correlation with rainfall in Angola, which is concentrated in March–April.

The analysis suggests a causality chain of atmospheric–oceanic anomalies. Variations of westward wind stress on the western equatorial Atlantic constitute an early link in this chain. The annual cycle is characterized by a relaxation of the wind stress from September–November to February–March. Anomalous seasonal relaxation of easterly wind stress over the western equatorial Atlantic remotely forces the sea surface temperature (SST) departures in the eastern South Atlantic, a large relaxation being followed by positive SST departures. Sea surface temperature modulates the rainfall over downstream Angola by controlling the atmospheric moisture and stability. Within each link of this causality chain, a substantial portion of the variance stems from processes other than the direct line wind stress → SST → rainfall.

1. Introduction

Research in the course of the past decade has progressed from a statistical description of climate anomalies and teleconnections toward the identification of mechanisms of interannual variability in the atmosphere–ocean system. It has become apparent that the coupling between hydrosphere and atmosphere is essential for the understanding of long-term variations (Davis, 1976; Hastenrath, 1976, 1978; Hastenrath and Heller, 1977; Barnett, 1977; Covey and Hastenrath, 1978; Lamb, 1978a,b) and that the ocean may respond to a *remote* forcing by the atmosphere (Wyrtki, 1975; Hurlburt *et al.*, 1976; McCreary, 1976; Adamec and O'Brien, 1978; Moore *et al.*, 1978; Servain *et al.*, 1982). Mechanisms of atmospheric forcing and hydrospheric response analogous to the Pacific El Niño phenomenon have been suggested for the Atlantic (Hisard, 1980; Merle, 1980; Merle *et al.*, 1980). Stretching as it does along the eastern extremity of the tropical South Atlantic, the Angola littoral appears an obvious corollary to the El Niño region of the South American West coast. As a further similarity, local meteorologists in Angola have long been aware of the tendency for abundant rainfall years to coincide with anomalously warm coastal waters (Queiroz, 1955; Staff of Serviço Meteorológico de Angola, Luanda, personal communication, 1971).

Thus, investigations into the general circulation causes of extreme climatic events in the Angola region offer the prospect of elucidating mechanisms of large-scale atmosphere–hydrosphere interaction in the tropical Atlantic. This is the motivation for the present study. Empirical analysis must by necessity proceed from effect to cause, that is, following the causality chain in an "upstream" direction. Various links in the chain of causality are substantiated successively in various sections of this paper. In the closing section, a continuous causality chain will be discussed, ranging from large-scale atmospheric circulation changes to air–sea coupling in the Atlantic Ocean and rainfall anomalies on the Angola coast.

2. Observations

Ship observations over the tropical Atlantic between 30°N and 30°S during the period 1911–72, stemming from the TDF-11 deck of the National Climatic Center at Asheville, North Carolina, have been processed by 1° square areas (Hastenrath and Lamb, 1977; Hastenrath and Heller, 1977), and subsequently compiled into 5° square values. Only the record of 1948–72 is used in the present study, data for the period 1940–47 being sparse. Elements of interest here include sea level pressure (SLP), zonal (u) and meridional (v) components of wind, sea surface temperature (SST), and total cloudiness. The density of ship observations is illustrated in Fig. 1.

Time series of individual monthly rainfall at Luanda, Lobito, and Moçámedes along the Angola coast (Fig. 1) for the period 1940–75 were obtained

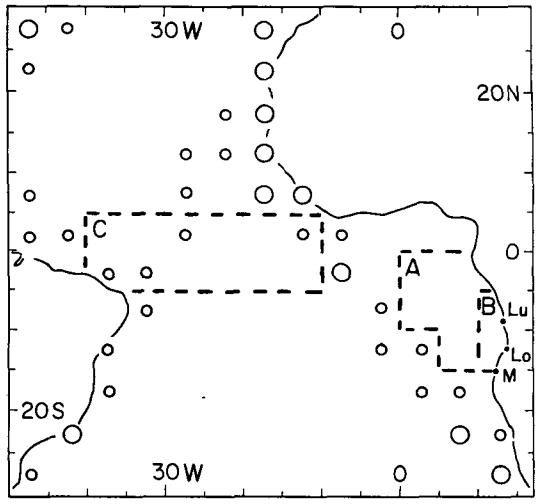

FIG. 1. Orientation map. Open circles denote stations on the Angola coast: Luanda (Lu), Lobito (Lo), and Moçâmedes (M). Atlantic areas A, B, and C are outlined by broken lines. Large and small open circles indicate, respectively, five degree squares with >30 000, and 30 000–12 000 observations during 1948–72.

from the Serviço Meteorológico de Angola, Luanda, and from U.S. Weather Bureau (1959), Environmental Sciences Service Administration, ESSA, (1967), and U.S. Weather Bureau, ESSA, NOAA (1956–80). The latter publication also contains upper-air observations for Luanda.

3. Background circulation and climate

Reference is made to the atlas of surface circulation and climate (Hastenrath and Lamb, 1977) which is based on long-term ship observations described in Section 2, and to the charts in Jackson (1964), Thompson (1965), Atkinson and Sadler (1970), and Hastenrath (1974). The SLP field over the Atlantic is dominated by two subtropical highs separated by a near-equatorial belt of low pressure. These features vary seasonally in intensity and position. In particular, the near-equatorial trough is deepest and reaches its southernmost, always northern hemispheric, location around March–April, while it attains its northernmost position and highest central pressure during July–September. The southeast trades and equatorial easterlies are weakest during January–March and strongest in June–September. The SST field shows a perennial east-to-west gradient in the South Atlantic, reflecting the cold Benguela and warm Brazil currents. Surface waters near the equator and in much of the tropical South Atlantic are coldest around August, and warmest around March–April.

Broadly paralleling the offshore SST variations, the march of the seasons along the Angola coast is characterized by a concentration of rainfall in March–April and an apex of the long dry season around June–August. Mean winds near the Angola coast are approximately southwesterly throughout the year, and thus parallel to the Southern Angola coast and onshore further north. Wind speed varies comparatively little in the course of the year, except for a brief July–September minimum.

4. Rainfall variability at the Angola coast

Annual (July to June) totals during 1940–75 at the three coastal stations show strong spatial correlation. Mean and standard deviation of annual rainfall were calculated for each station, and the annual rainfall expressed as normalized departure from the mean. The three-station average of normalized departure (Fig. 2) serves as a robust index of rainfall activity in coastal Angola. The annual ranfall is narrowly concentrated in March–April (see Fig. 11). Fig. 2 illustrates the pronounced interannual variability of rainfall. Within the 1948–72 period, the most extreme years on the Angola coast were identified from Fig. 2 as follows: 1948 (i.e., July 1947–June 1948), 53, 54, 58, 64, 72 as DRY; and 1957, 62, 63, 69, 71 as WET. The March–April rainfall on the Angola coast during each DRY and WET year was similarly well below or above average. Maps of large-scale atmospheric and oceanic fields were constructed for composites of these extremely dry and wet years along the Angola coast, as discussed in Sections 5–7.

5. Atmospheric–oceanic departure patterns during the Angola rainy season

Anomalous circulation features over the Atlantic coincident with an extreme rainy season on the Angola coast are illustrated in Figs. 3 and 4 by March–April charts composited for the six DRY and the five WET years (Section 4), respectively, in terms of de-

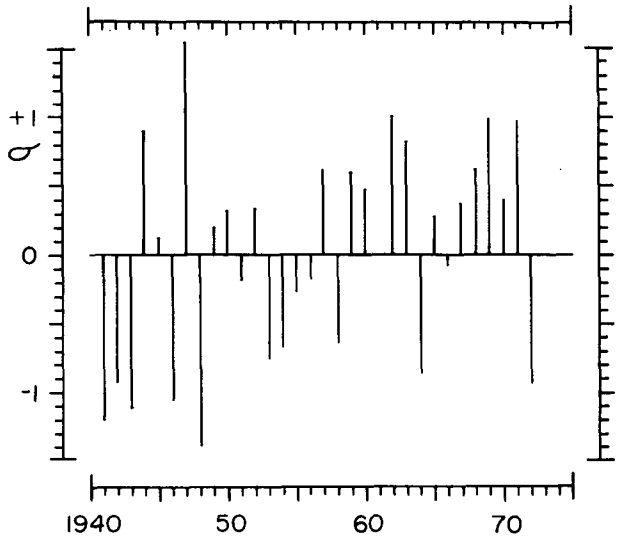

FIG. 2. Time series plot of Angola coast rainfall index (σ).

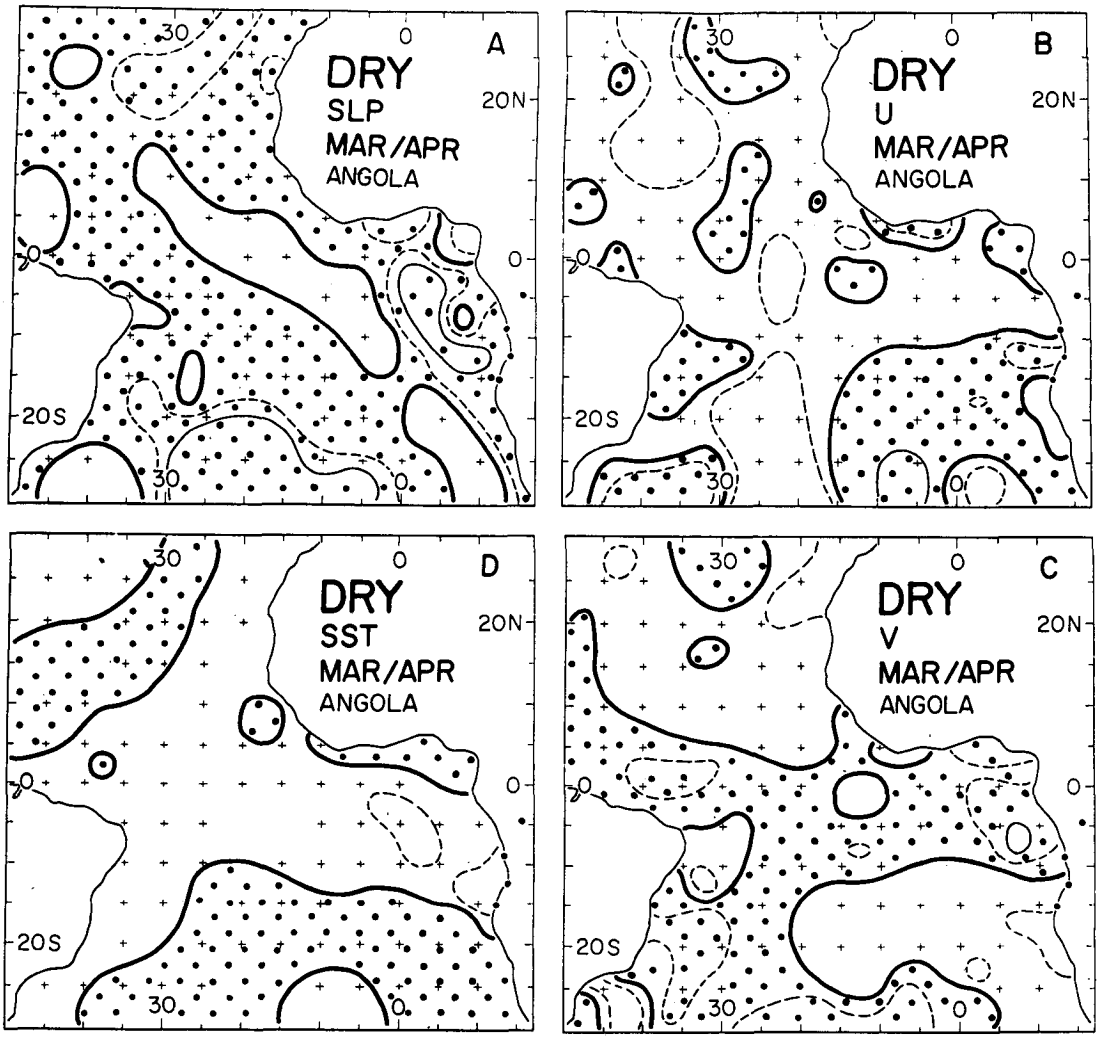

FIG. 3. March–April composites of the six DRY years (1948, 53, 54, 58, 64 and 72) on the Angola coast expressed as departure from the 25 year (1948–72) mean pattern. Dot raster denotes areas of positive departure, zero line (heavy), and isolines at 1.0 units (solid), and at 0.5 (broken). (A) sea level pressure SLP in mb, (B) u and (C) v components of surface wind in m s^{-1}, and (D) SST in °C.

partures from the 1948–72 mean. In addition, Fig. 5 shows the spatial patterns of correlation between the Angola coastal rainfall index and March–April values of SLP, u and v wind components and SST.

During the composite DRY rainy season (Fig. 3), positive SLP departures occur near the Angola coast and over much of the South Atlantic. Meanwhile the trades are weak over the southeast Atlantic poleward of 10°S, especially off the coast of Southwest Africa. Winds are strong over much of the equatorial Atlantic. SST departures are negative in a band extending from the Angola coast into the open equatorial Atlantic.

Fig. 4 shows that departure patterns during the composite WET rainy season are approximately inverse to those described above for DRY; the Southeast Atlantic trades are greatly enhanced, and positive SST anomalies prevail in most of the tropical Atlantic, with largest values off the Angola coast.

The features borne out by stratification in Figs. 3 and 4 are further reflected in the correlation maps (Fig. 5). Positive rainfall departures at the Angola coast tend to be associated with: negative SLP anomalies over the central and Western South Atlantic, enhanced trades in the Southeastern Atlantic but reduced winds elsewhere in the equatorial and South Atlantic, and anomalously warm waters especially across the equatorial Atlantic. In particular, SST is higher and SLP lower near the Angola coast.

Figs. 3–5 indicate a strong association between Angola coast rainfall and offshore SST within the area marked A in Fig. 1. Further evaluations corroborate this coupling. Thus, the Angola coast rainfall index and SST in area A (see Fig. 1) are correlated at +0.60;

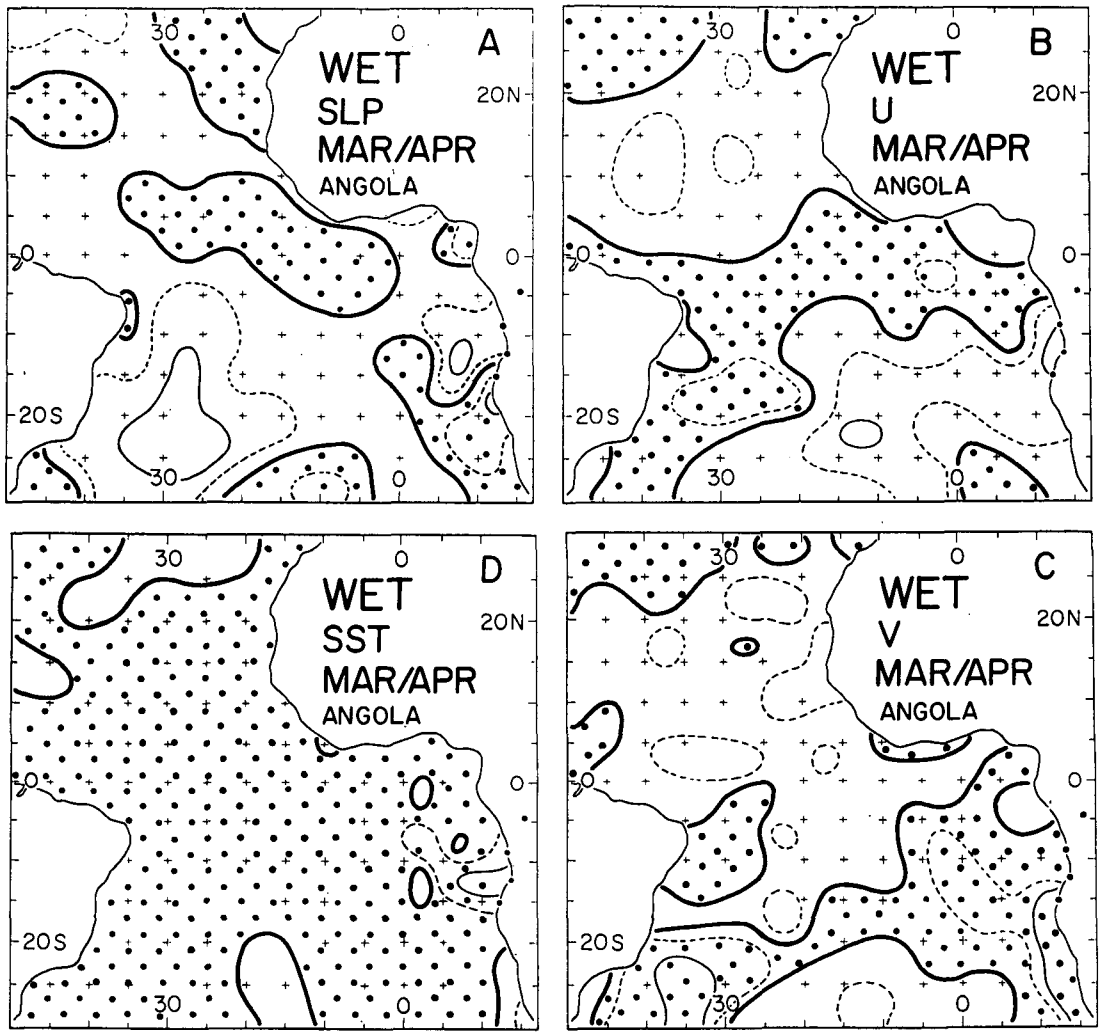

FIG. 4. As in Fig. 3 but for the five WET years (1957, 62, 63, 69 and 71).

all five DRY rainy seasons have negative SST departures, while four of the five WET rainy seasons are coincident with positive SST departures. Figures 3–5 are in part reminiscent of the latitudinal shift of circulation systems identified by Lamb (1978a,b) as characteristic of rainfall anomalies in Subsaharan Africa, although there is no one-to-one relationship between extreme hydrometeorological events in the two regions.

6. Coupling mechanisms between SST and rainfall anomalies

A positive correlation was found in Section 5 between rainfall on the Angola coast and SST in the adjacent ocean. In an effort to explore an immediate link in a long causality chain, two mechanisms of SST–rainfall coupling are hypothesized here: 1) SST controls the moisture in the lower atmosphere downwind over the coast; and 2) SST affects the actual and convective stability of the lower atmosphere downwind over the coast, in each case influencing the likelihood and intensity of coastal precipitation. These hypotheses are examined in Table 1.

If mechanism 1 links coastal rainfall to SST, positive correlations should be observed between coastal rainfall and moisture in the lower troposphere, and between the latter and SST upwind. Moisture is represented by surface values of March–April mixing ratio at Luanda. Patchy mixing ratio series for Lobito and Moçâmedes are not used here. Table 1 indicates a positive correlation between coastal rainfall and the mixing ratio. March–April values of SST departure averaged for area B off the Angola coast (Fig. 1) represent SST upwind from Luanda. Table 1 indicates a positive correlation between upwind SST departure and the Luanda mixing ratio. These positive correlations are consistent with the hypothesis that mech-

anism 1 links coastal rainfall to SST. Note that the observed correlations could arise if increased precipitation causes the surface air to be more moist and if the precipitation is related to SST by some other mechanism. The problem of cause and effect cannot be resolved from the data available.

We now investigate the validity of mechanism 2. The March–April lapse rate between the surface and 700 mb at the Luanda radiosonde station is the stability indicator to be used here. Table 1 indicates a positive correlation between the lapse rate and rainfall. Meanwhile, the lapse rate and the upwind SST are shown in Table 1 to be positively correlated. Tables 1 and 2 show strong positive correlations of the March–April surface air temperature at Luanda with the rainfall index and with upwind SST, while negligible correlation is apparent between the 700 mb temperature at Luanda and the rainfall index. These results indicate that low stability due to warm surface air is coincident with high SST and abundant rainfall; hence they support the hypothesis that mechanism 2 links coastal rainfall to SST.

The March–April lapse rate of equivalent potential temperature between the surface and 700 mb at Luanda is used to indicate convective instability. The positive correlation of this lapse rate with rainfall and upwind SST displayed in Table 1 suggests that increased convective instability is coincident with high SST and abundant rainfall as expected in the operation of mechanism 2.

To summarize: The results presented here are consistent with the hypothesis that SST affects rainfall on the Angola coast by controlling the moisture and stability of the lower troposphere (mechanism 2).

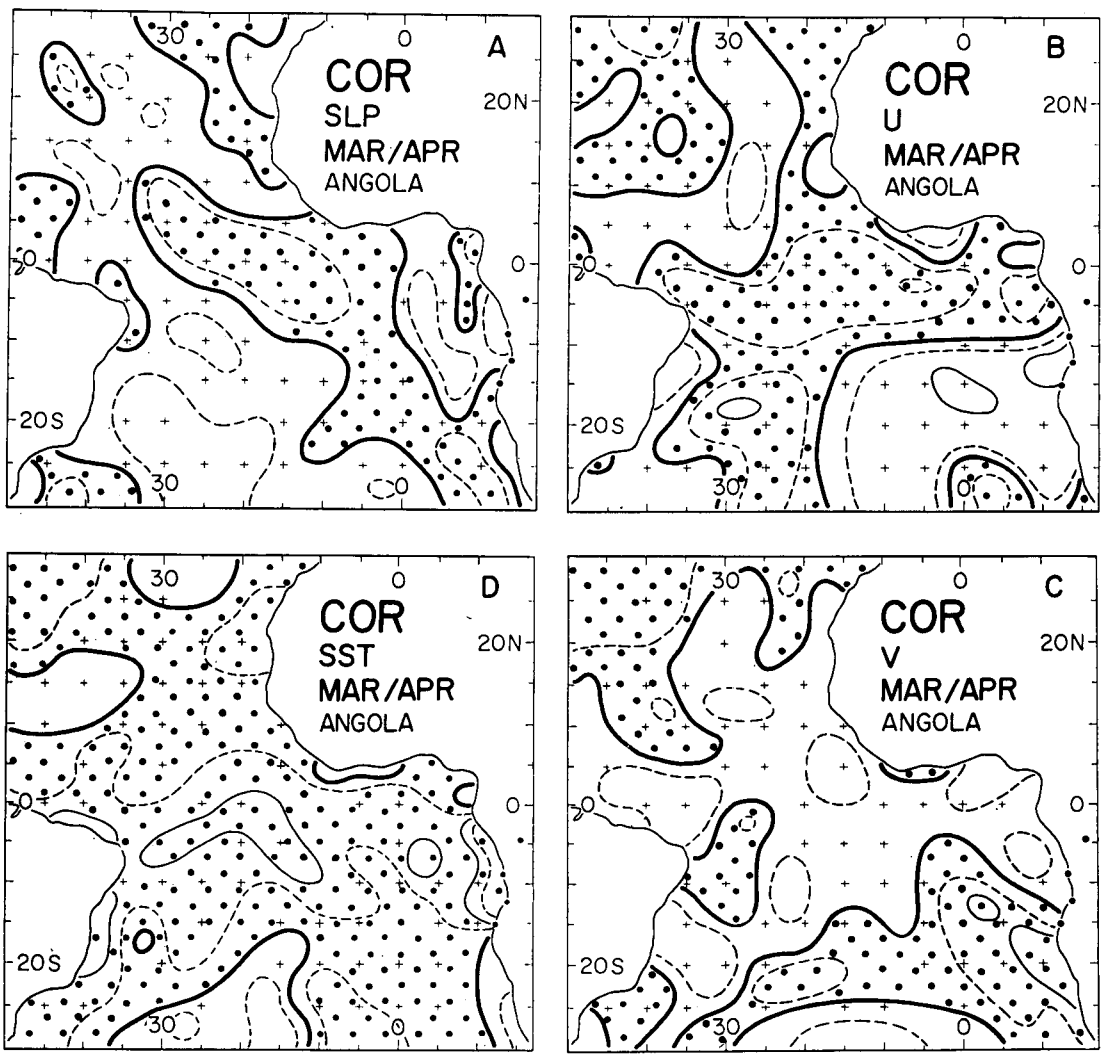

FIG. 5. Isocorrelates of Angola coast rainfall index versus March–April values of indicated elements in 5 degree blocks over the Atlantic during 1948–72. Dot raster denotes areas of positive values, zero line is heavy, and isocorrelates at 0.4 (solid) and at 0.2 and 0.6 (broken). (A) SLP, (B) u, and (C) v components of surface wind and (D) SST.

TABLE 1. Correlation coefficients, in hundredths, between Angola coast rainfall index and March–April values of various atmospheric and oceanic parameters. Symbols for variables in columns I and II are as follows:

ΔSST(A)	SST departure in area A
ΔSST(B)	SST departure in upwind area B
m	mixing ratio at Luanda
γ	lapse rate of virtual temperature, surface to 700 mb, at Luanda
γ_e	lapse rate of equivalent potential temperature, surface to 700 mb at Luanda
T_s	surface air temperature at Luanda
T_{700}	700 mb air temperature at Luanda
$C1$	cloudiness in area 5–10°S, 10–15°E
$C2$	cloudiness in area 10–15°S, 10–15°E
R year	July–June Angola coast rainfall index
R(A–J)	August–January Angola coast rainfall index
R(F–M)	February–May Angola coast rainfall index.

One, two, and three asterisks denote significance at the 10, 5 and 1% levels, respectively. Quenouille's (1952, p. 168) method was used to account for the reduction of effective degrees of freedom due to persistence.

I	II	Correlation coefficient	Years	Period
ΔSST(A)	R year	+60***	23	1948–72
m	R year	+56**	20	1956–75
m	ΔSST(B)	+46	13	1956–72
m	γ	+59	13	1956–72
γ	R year	+40	16	1956–75
γ	ΔSST(B)	+52	10	1956–71
γ_e	R year	+42	12	1956–72
γ_e	ΔSST(B)	+34	12	1956–72
T_s	R year	+63***	20	1956–75
T_s	ΔSST(B)	+77***	13	1956–72
T_{700}	R year	−05	16	1956–75
R(A–J)	R(F–M)	+10	35	1941–75

7. Atmospheric–oceanic departure patterns preceding the Angola rainy season

Conditions over the Atlantic prior to an extremely WET rainy season on the Angola coast are indicated by Fig. 6, which shows correlations between the Angola coast rainfall index and September–October Atlantic circulation elements. The correlation patterns suggest that six months before a WET rainy season, pressure departures tend to be negative in a belt extending from the Angola coast into the interior of the South Atlantic and in the western equatorial Atlantic, but positive in most other regions, and especially in the eastern equatorial Atlantic. Associated with this pattern are strong easterlies over much of the map area and in particular over the western equatorial Atlantic. Positive SST anomalies appear along the Angola coast, as during a WET rainy season (Figs. 4 and 5). Figs. 4–6 suggest no simple causal relationship between the variations of meridional wind component and SST off the Angola coast. Table 1 shows that extreme rainfall during the pre-season is only a weak predictor of extreme rainfall during the principal rainy season.

Continuing the pattern comparison in Figs. 4 and 5 we note that the easterly wind component over the equatorial Atlantic is weak during March–April of a WET rainy season, while the reverse pattern deviations prevail six months previously. This condition will be considered further in Section 8.

8. Causes of SST and SLP anomalies off the Angola coast

Extreme rainfall on the Angola coast has been shown in Section 5 to coincide with anomalous atmosphere–ocean conditions in much of the tropical Atlantic, in particular with pronounced SST departures off the Angola coast (Figs. 3–5). Evidence has been presented in Section 6 to the effect that SST affects rainfall through variations of atmospheric moisture and stability. Proceeding upstream in the chain of causalities, the present section aims at elucidating the forcings that produce the SST departures over the eastern South Atlantic. To this end, four hypotheses are examined in the following: 1) SLP anomalies induced by SST departures through hydrostatic adjustment, 2) SST anomalies related to local cloudiness, 3) SST anomalies resulting from local wind speed, and 4) SST anomalies due to remote wind stress forcing.

a. SLP anomalies induced by hydrostatic adjustment

The hypothesis is made that SLP departures observed off Angola during the composite WET and DRY rainy seasons result from hydrostatic adjustment to the underlying SST departures then observed. A calculation is performed to determine if a change in air temperature of similar magnitude to the difference in SST between the DRY (Fig. 3) and WET (Fig. 4) composites could cause a change in SLP of the same order of magnitude as the observed difference in SLP between the DRY and WET composites. March–April SST and SLP departures for individual 5 degree square areas were evaluated with the assumption that the height of the 700 mb surface is unaffected by the temperature pattern in the underlying air column. It is concluded that the higher SST associated with increased Angola precipitation may

TABLE 2. Correlation coefficients (hundredths) between March–April SST, cloudiness C, and wind speed V over area A (see Fig. 1) during months indicated. Period 1948–72. None significant at the 10% level.

Months	C	V
Jan–Feb	+17	+26
Feb–Mar	−12	−34
Mar–Apr	−04	−38
Apr–May	+11	+01
May–Jun	+04	+02

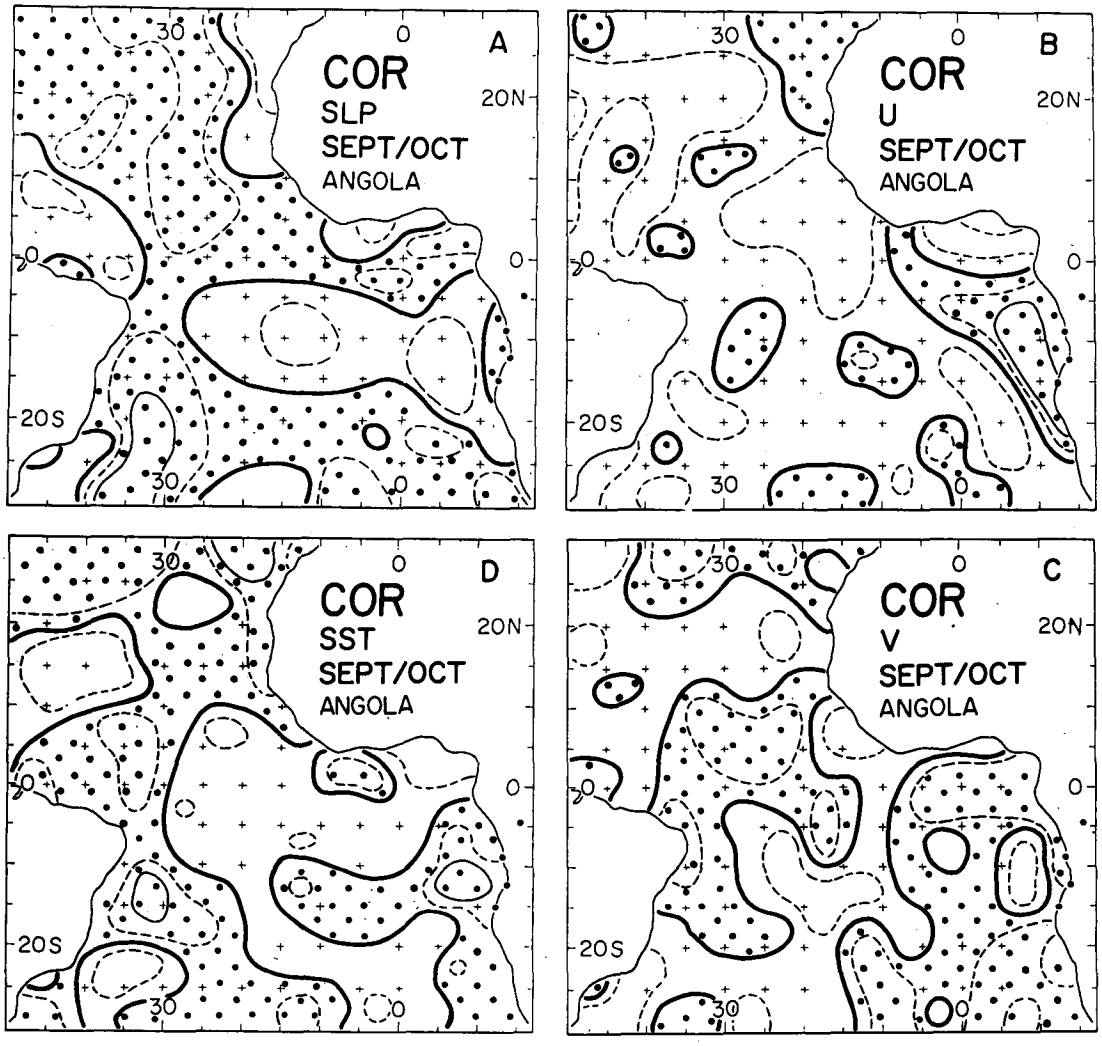

FIG. 6. As in Fig. 5 but for September–October.

heat the lower troposphere locally, thus inducing lower SLP by hydrostatic adjustment.

b. SST anomalies related to local cloudiness

The hypothesis is made that negative (positive) cloudiness departures force the development of positive (negative) SST departures by controlling the insolation at the ocean surface. Then, negative correlations should be observed for March–April SST versus prior and/or coincident cloudiness. Fig. 7 shows isocorrelates for March–April SST versus local March–April cloudiness over the Atlantic Ocean. Negative correlations are found over most of the South Atlantic while positive correlations occur near the trade wind discontinuity. This pattern may be caused by clouds near the trade wind discontinuity being mainly convective in origin, while the clouds over at least the southeast Atlantic are stratiform, forming within the subsidence inversion present there (Hastenrath and Lamb, 1977). It is suggested that underlying warmer waters enhance convective activity and thus cloudiness near the trade wind discontinuity, while warmer waters in the South Atlantic weaken the trade wind inversion which in turn acts to disperse the stratiform clouds. Another possibility in the South Atlantic is that reduced cloudiness may be responsible for the approximately concurrent higher SST through the hypothesized mechanism of increased insolation. A combination of these two mechanisms gives the possibility of positive feedback.

In the vicinity of the Angola coast, positive correlations are apparent immediately adjacent to the coast, but there is no consistent tendency over area A. Table 2 shows that March–April SST in area A is negatively correlated with both the February–March and March–April, but not the April–May cloudiness departures. These correlations are weak,

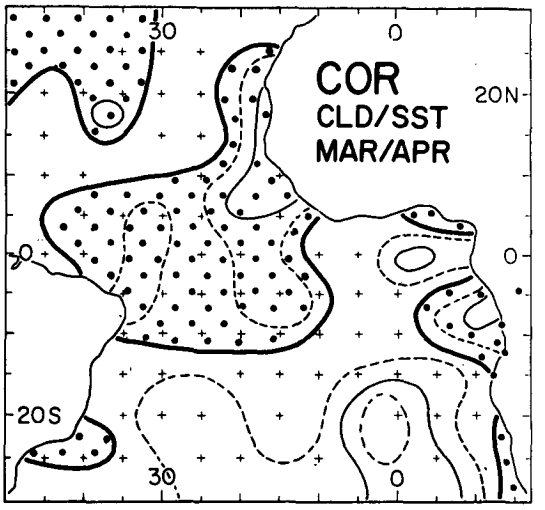

FIG. 7. Isocorrelates of March–April SST and cloudiness. Symbols as in Fig. 5.

but do suggest that reduced cloudiness leads higher SST. Cloudiness in area A prior to, during, and after the composite DRY and WET rainy seasons is shown in Fig. 8. The period of SST decrease observed prior to the composite DRY rainy season coincides with positive cloudiness departure; otherwise no clear tendency is apparent for fluctuations in cloudiness to lead opposite fluctuations in SST. Conditions during the WET are broadly inverse to those during the DRY composites. Figure 8 and Table 2 suggest that cloudiness may exert a weak influence on March–April SST off the Angola coast, and contribute to the negative SST departures present during the composite DRY rainy season.

An interesting observation from Fig. 8 is that anomalous rainfall on the Angola coast would not seem to be associated with large anomalies of the same sign in the offshore cloudiness. This is reminiscent of the conditions off Peru during El Niño where scattered but rainbearing cumuliform clouds replace the more usual continuous stratiform clouds.

c. *SST anomalies resulting from local wind speed*

The hypothesis is made that negative (positive) departures of wind speed might force the development of positive (negative) SST departures by modulating the rate of evaporation and sensible heat loss from the ocean surface and affecting the rate of turbulent mixing of surface waters with colder water from below. If so, negative correlations should be observed for March–April SST versus prior and/or coincident wind speed. Fig. 9 shows negative correlations between SST and local wind speed over most of the Atlantic and over most of area A. Table 2 shows SST in March–April to be negatively correlated with wind speed in February–March and March–April, but not April–May. This pattern suggests that stronger wind speeds tend to precede lower SST. Figure 8 indicates that the rapid fall in the SST departure observed prior to and during the composite DRY rainy season coincides with above average wind speed, but that wind speed remains near average when the SST departure is rising prior to and during the composite WET rainy season. In summary, local

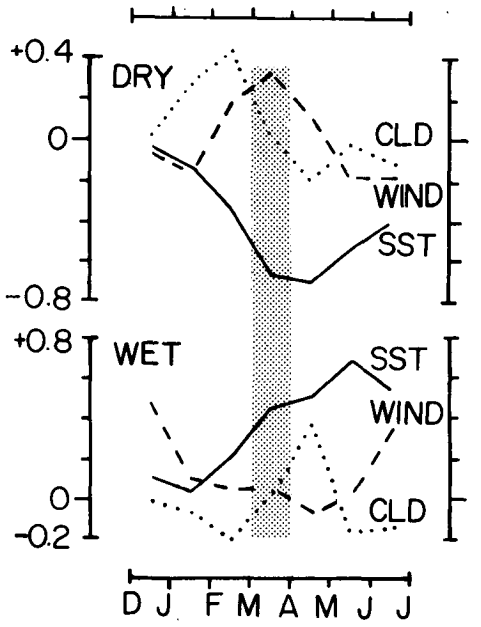

FIG. 8. Fluctuations of SST (solid, °C) and wind speed (broken, m s^{-1}) and cloudiness (dotted line, tenths) departures in area A (Fig. 1) during the composite DRY and WET years. Departures are bimonthly means (i.e., March–April, April–May, etc.). Typical standard errors are 0.2 m s^{-1} for wind speed, and 0.04 for cloudiness. Shading indicates the March–April rainy season.

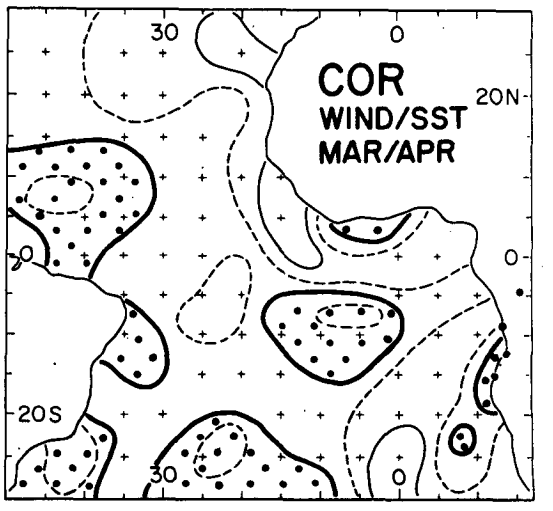

FIG. 9. As in Fig. 5 but for March–April SST and wind speed.

wind speed may have a significant influence on March–April SST off Angola. In particular, increased wind speed might contribute to the low SST observed during the composite DRY rainy season.

d. SST anomalies due to remote wind stress forcing

In searching for circulation features responsible for remote forcing of the SST near the Angola coast, refer first to Fig. 6. Six months prior to a WET rainy season on the Angola coast, easterlies over much of the Atlantic tend to be strong. Further, Figs. 4 and 5 indicate that strong easterlies are not evident in the central and western equatorial Atlantic during a WET rainy season. It is hypothesized that an anomalously large weakening of the easterlies, and hence of the westward wind stress on the central and Western equatorial Atlantic, induces the later appearance of anomalously warm waters off the Angola coast.

Wyrtki (1975), Hurlburt *et al.* (1976), and McCreary (1976) pioneered in the study of remote atmospheric forcing of the tropical Pacific Ocean. Katz *et al.* (1977), Adamec and O'Brien (1978), and Moore *et al.* (1978) expanded the theoretical treatment to the Atlantic. A correlation analysis by Servain *et al.* (1982) based on our data bank of long-term ship observations suggests that an anomalous weakening of the westward wind stress in the Western equatorial Atlantic precedes positive SST departures in the Gulf of Guinea by a few months. They relate this phenomenon to the remote forcing idea of Moore *et al.* (1978), according to which variations in the westward wind stress over the western equatorial Atlantic should induce SST fluctuations in the eastern equatorial Atlantic, with a subsequent propagation of wave disturbances poleward along the coasts in both hemispheres. In order to explore further the relation of southeast Atlantic SST anomalies to equatorial wind stress forcing, isocorrelate maps were constructed of March–April SST in area A (Fig. 1) and the zonal wind component in 5 degree square blocks of the Atlantic during 1) March–April and during 2) the preceding September–October, respectively. These maps are not reproduced here, because map 1) is an approximate replica of Fig. 5B, and map 2) closely resembles Fig. 6B. This underlines further that positive (negative) SST departures in area A during March–April tend to be preceded by anomalously strong (weak) easterlies over the western and central equatorial Atlantic half a year earlier, and that they coincide with anomalously weak (strong) easterlies over the equatorial Atlantic in March–April.

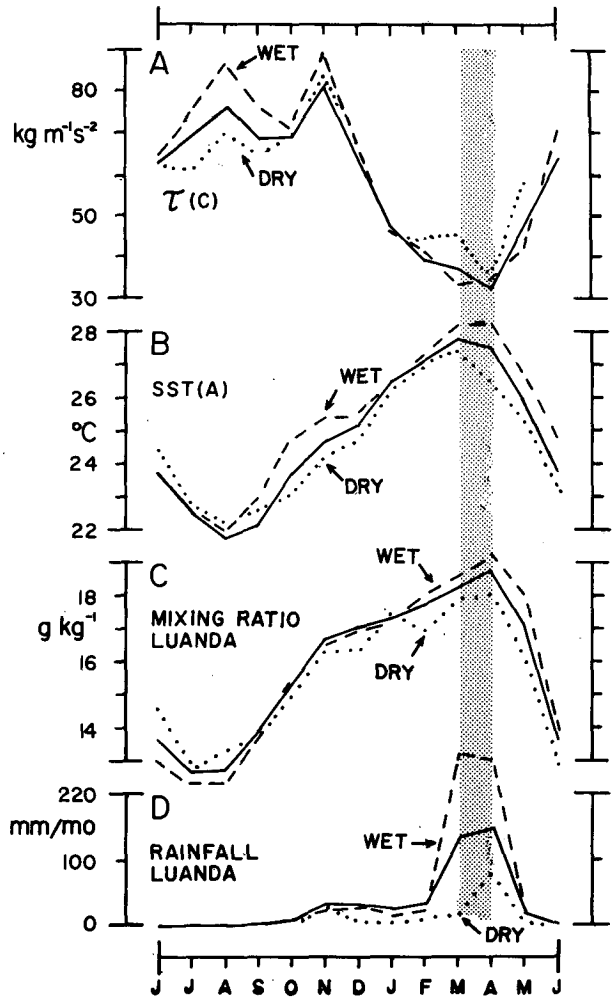

FIG. 11. Annual march of (A) westward wind stress in area C, (B) SST in area A, (C) surface mixing ratio at Luanda, (D) rainfall at Luanda (see Fig. 1.). Solid, dashed, and dotted lines refer to the 1948–72 average and the WET and DRY composites, respectively.

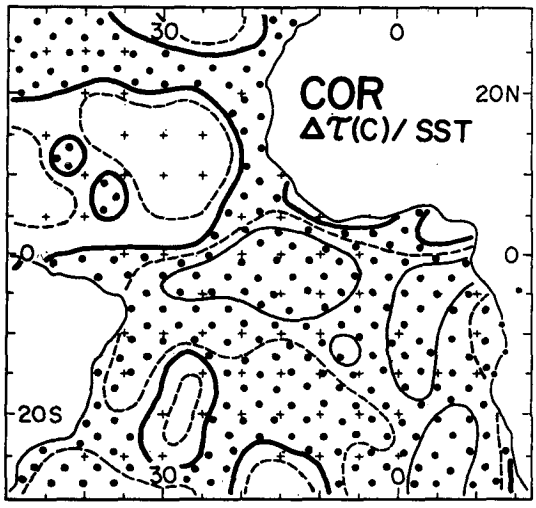

FIG. 10. Isocorrelates of seasonal wind stress relaxation in area C (see Fig. 1) versus February–April SST in 5 degree square blocks of the Atlantic during 1948–72. *Seasonal wind stress relaxation* is defined as September–November westward wind stress minus the February–April westward wind stress. Symbols as in Fig. 5.

The above results point towards the importance of the seasonal *relaxation* of zonal wind stress along the Atlantic equator for the origin of SST anomalies off the Angola coast. Therefore, the following analysis summarized in Figs. 10 and 12, focuses on the seasonal relaxation of equatorial wind stress directly. Time series of westward wind stress were constructed for area C (Fig. 1) and for subareas of this 5°N–5°S band to the west and east of 40°W, respectively. The annual march of westward wind stress in area C is plotted in part A of Fig. 11, separately for the average of 1948–72, and the DRY and WET composites. Plots for the two subareas of area C are similar and are not reproduced here. *Seasonal relaxation of westward wind stress* is here defined as the difference between the westward wind stress in September–November minus that in February–April. Figure 10 is an isocorrelate map of this quantity in area C versus March–April SST in 5° square blocks of the tropical Atlantic. Fig. 10 shows strong positive correlations for the southeastern Atlantic. Maps constructed with reference to the two subareas of area C are similar, but are not reproduced here. On the whole, correlations are strongest with respect to the entire area C and least with respect to the eastern subarea. These results are consistent with the hypothesis of remote wind stress forcing of SST anomalies off the Angola coast.

Fig. 11 further illustrates the evolution of equatorial wind stress departures, and of anomalies of SST, specific humidity and rainfall in the southeast Atlantic–Angola sector. In panel A of Fig. 11, the annual march of equatorial wind stress (area C) appears amplified during the WET, and reduced for the DRY Angola composite. Similarly, SST anomalies off the Angola coast (part B of Fig. 11) during the WET and DRY composites appear as enhancements and suppressions of the average annual cycle. The same is true for the atmospheric humidity and rainfall at the coast (parts C and D of Fig. 11). Thus Fig. 12 not only supports the wind stress hypothesis proposed in the present section, but also lends further credence to the hypothesis of SST influencing rainfall through variations of atmospheric moisture, as discussed in Section 6.

Table 3 summarizes the spatial correlations pertinent to the remote forcing mechanism. Both SST in area A (Fig. 1) and Angola rainfall are significantly correlated with the seasonal relaxation of zonal wind stress in the western equatorial Atlantic (area C in Fig. 1). That the *relaxation* of wind stress rather than the wind stress itself is important in this mechanism is underlined by the very weak correlation between SST in area A and the contemporaneous wind stress in area C (Table 3).

These results are interesting in relation to the paper by Servain *et al.* (1982), who found a teleconnection between zonal wind stress (rather than *relaxation* of wind stress) over the western equatorial Atlantic and SST in the Gulf of Guinea. The following details may merit attention in a comparison between the two studies: 1) it is plausible that weak wind stress is related to a *relaxation* of wind stress in the time interval immediately preceding, but Servain *et al.* (1982) did not examine the *relaxation* of wind stress; 2) their time series analyses make no specific distinction of seasons; and 3) as SST response region they studied the Gulf of Guinea but not the waters off Angola. Further empirical investigations are intended of the wind forcing and SST response in the equatorial and South Atlantic. In this context it is noted that the theoretical model studies of Hurlburt *et al.* (1976)

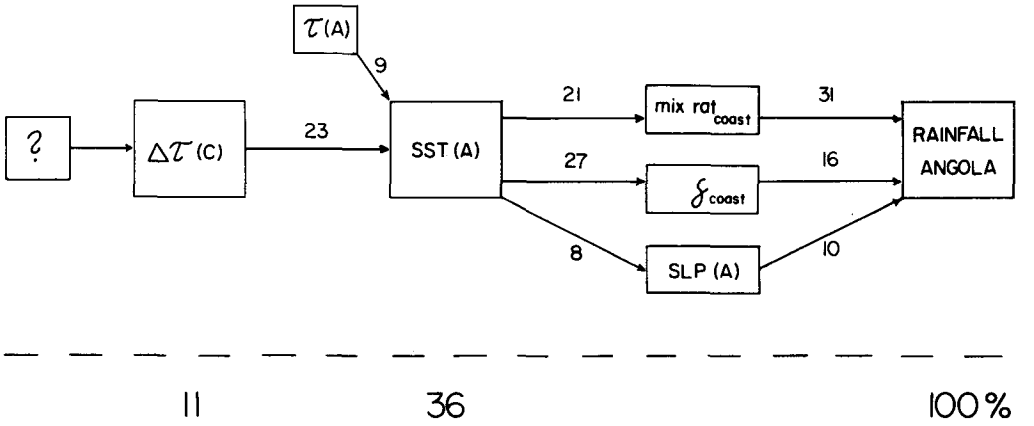

FIG. 12. Causality-chain of atmospheric–oceanic anomalies; $\Delta\tau$(C) is SON − FMA difference of westward wind stress in area C (Fig. 1), τ(A) is total wind stress in area A (Fig. 1), SST(A) the SST in area A, mix rat_{coast} the mixing ratio at Luanda, γ_{coast} the sfc − 700 mb temperature difference at Luanda and SLP(A) is sea level pressure in area A. Numbers next to the arrows signify percentage of variance in the downstream element explained by the upstream element. Numbers at bottom of graph are percentage of variance of Angola coast rainfall explained by element in box above. (Source: Table 3).

TABLE 3. Correlation coefficients in hundredths between indicative parameters. Symbols for variables in columns I and II as follows:

R year	July–June Angola coast rainfall index;
SST(A)	February–April sea surface temperature in area A (see Fig. 1).
SLP(A)	February–April sea level pressure in area A.
τ(A)	February–April total wind stress in area A.
τ(C)	January–March westward wind stress in area C.
$\Delta\tau$(C)	September–November minus February–April westward wind stress in area C.
SOI, MAM	Southern Oscillation index for March–April–May (Wright, 1975, 1977).

One, two and three asterisks indicate significance at the 10, 5, and 1% levels, respectively. Quenouille's (1952, p. 168) method was used to account for the reduction of effective degrees of freedom due to persistence.

I	II	Correlation coefficient	Years	Period
τ(A)	SST(A)	−30	22	1948–72
τ(C)	SST(A)	−5	23	1948–72
$\Delta\tau$(C)	SST(A)	+47**	23	1948–72
$\Delta\tau$(C)	*R* year	+33	25	1948–72
SLP(A)	*R* year	+31	23	1948–72
SLP(A)	SST(A)	−28	23	1948–72
SOI, MAM	*R* year	+28	34	1941–74

and McCreary (1976) point to the possible important role of wind stress *relaxation* in the remote forcing of SST.

Table 3 further shows that SST in area A is also affected by the local wind stress, but to a lesser extent than by the remote forcing. An isocorrelate map of wind stress in area A versus SST in the Atlantic (not reproduced here) shows a negative correlation (of about −0.4) within a few degrees of the Angola coast. There is a weak negative correlation between Angola rainfall and SLP in area A, which in turn may be to a large extent hydrostatically controlled by the local SST.

In an attempt to relate events in the Atlantic sector to the global tropics, correlation coefficients were calculated with Wright's (1975, 1977) Southern Oscillation Index (SOI). A weak positive correlation was found between Angola coast rainfall and the SOI (Table 3). However, wind stress relaxation and the SOI were found to be essentially uncorrelated.

9. Causality chain of anomalies

In Sections 6 and 8, various causal linkages were substantiated, proceeding always from effect to cause, that is, in the *upstream* direction. In this closing section, a complete causality chain will be considered with reference to Fig. 12, and this can now be undertaken with a *downstream* perspective.

Whatever the causes of anomalous seasonal relaxation of wind stress in the western equatorial Atlantic, this makes for 23% of the SST variance off the Angola coast, while the local wind forcing contributes only 9%. The SST variations over the eastern South Atlantic in turn—presumably via atmospheric moisture and stability—accounts statistically for 36% of the rainfall variability along the Angola coast. Sea level pressure over the eastern South Atlantic may exert an effect on Angola rainfall through particulars of the atmospheric flow pattern. Moreover, the pressure itself may in part be hydrostatically controlled by the local SST. Atmospheric moisture and stability are correlated; a two-way effect-cause relationship seems plausible between moisture and rainfall. It is noted that within each link of the causality chain, a substantial portion of the variance stems from processes other than the line wind stress → SST → rainfall. This notwithstanding, the present study documents a long chain of causes and effects, ranging from mechanical forcing in the remote western equatorial Atlantic to extreme climatic events on the African continent.

Acknowledgments: This study was supported by NSF Grants ATM79-11131, ATM82-00511 and LOE 81-20583. J. McCreary, Nova University, J. Young and D. Johnson, University of Wisconsin, offered helpful suggestions. S. H. acknowledges conversations with the Staff of the Serviço Meteorológico de Angola, Luanda, in 1971, and with colleagues of the SEQUAL and FOCAL programs in 1980–82.

REFERENCES

Adamec D., and J. J. O'Brien, 1978: The seasonal upwelling in the Gulf of Guinea due to remote forcing. *J. Phys. Oceanogr.*, **8,** 1050–1060.

Atkinson, G. D., and J. C. Sadler, 1970: Mean-cloudiness and gradient-level wind charts over the tropics. Air Weather Service Tech. Rep. 215, Vol. 2.

Barnett, T. P., 1977: An attempt to verify some theories of El Niño. *J. Phys. Oceanogr.*, **7,** 633–647.

Covey, D. C., and S. Hastenrath, 1978: The Pacific El Niño phenomenon and the Atlantic circulation. *Mon. Wea. Rev.*, **106,** 1280–1287.

Davis, R. E., 1976: Predictability of sea surface temperature and sea level pressure anomalies over the North Pacific Ocean. *J. Phys. Oceanogr.*, **6,** 249–266.

Environmental Science Service Administration, 1967: *World Weather Records 1951–1960.* Vol. 5: *Africa.* U.S. Government Printing Office, Washington, DC, 574 pp.

Hastenrath, S., 1974: On the upper-air circulation over Angola. *Bonn. Meteor. Abh.*, **16,** 353–360.

——, 1976: Variations in low-latitude circulation and extreme climatic events in the tropical Americas. *J. Atmos. Sci.*, **33,** 202–215.

——, 1978: On modes of tropical circulation and climate anomalies. *J. Atmos. Sci.*, **35,** 2222–2231.

——, and L. Heller, 1977: Dynamics of climatic hazards in northeast Brazil. *Quart. J. Roy. Meteor. Soc.*, **103,** 77–92.

——, and P. J. Lamb, 1977: *Climatic Atlas of the Tropical Atlantic and Eastern Pacific Oceans.* The University of Wisconsin Press, 113 pp.

Hisard, P., 1980: Observation de réponse de type "El Niño" dans l'Atlantique tropical oriental—Golfe de Guinée. *Ocean. Acta,* **3,** 69–78.

Hurlburt, H. E., J. C. Kindle and J. J. O'Brien, 1976: A numerical simulation of the onset of El Niño. *J. Phys. Oceanogr.*, **6**, 621–631.

Jackson, S. P., 1964: *Climatic Atlas of Africa.* Government Printer, Pretoria, 117 pp.

Katz, E. J., and collaborators, 1977: Zonal pressure gradient along the equatorial Atlantic. *J. Mar. Res.*, **35**, 293–307.

Lamb, P., 1978a: Case studies of tropical Atlantic surface circulation pattern during recent Sub-Saharan weather anomalies. *Mon. Wea. Rev.*, **106**, 482–491.

——, 1978b: Large-scale tropical Atlantic surface circulation patterns associated with Sub-Saharan weather anomalies. *Tellus*, **30**, 240–251.

McCreary, J., 1976: Eastern tropical ocean response to changing wind systems, with application to El Niño. *J. Phys. Oceanogr.*, **6**, 632–645.

Merle, J., 1980: Variabilité thermique annuelle et interannuelle de l'Océan Atlantique équatorial Est. L'hypothèse d'un "El Niño" Atlantique. *Ocean. Acta*, **3**, 209–220.

——, M. Fieux and P. Hissard, 1980: Annual signal and interannual anomalies of sea surface temperatures in the Eastern equatorial Atlantic Ocean. *Deep Sea Res.*, GATE (Suppl. II) **26**, 77–102.

Moore, D. W., P. Hisard, J. McCreary, J. Merle, J. J. O'Brien, J. Picaut, J. M. Verstraete and C. Wunsch, 1978: Equatorial adjustment in the eastern Atlantic. *Geophys. Res. Lett.*, **5**, 637–640.

Queiroz, D. X., 1955: Variabilidade das chuvas em Angola. Serviço Meteorológico de Angola, Luanda, 29 pp.

Quenouille, M. H., 1952: *Associated Measurements.* Butterworths, 242 pp.

Servain, J., J. Picaut and J. Merle, 1982: Evidence of remote forcing in the equatorial Atlantic Ocean. *J. Phys. Oceanogr.*, **12**, 457–469.

Thompson, B. W., 1965: *The Climate of Africa.* Oxford University Press, 132 pp.

U.S. Weather Bureau, 1959: *World Weather Records 1941–50.* U.S. Government Printing Office, Washington, DC, 574 pp.

——, ESSA, NOAA, 1956–1980: *Monthly Climatic Data for the World,* Vols. 9–33, National Climatic Center, Asheville, N.C.

Wright, P. B., 1975: An index of the Southern Oscillation. Res. Pub. No. 4., Climatic Research Unit, University of East Anglia, 22 pp.

——, 1977: The Southern Oscillation—patterns, and mechanisms of the teleconnections and the persistence. HIG-77-13, Hawaii Institute of Geophysics, 107 pp.

Wyrtki, K., 1975: El Niño—the dynamic response of the equatorial Pacific Ocean to atmospheric forcing. *J. Phys. Oceanogr.*, **5**, 572–584.